PHYSICAL REVIEW D VOLUME 8, NUMBER 11 1 DECEMBER 1973

Measurement of Delbrück Scattering and Observation of Photon Splitting at High Energies

G. Jarlskog* and L. Jönsson
University of Lund, Lund, Sweden

S. Prünster, H. D. Schulz, H. J. Willutzki, and G. G. Winter
Deutsches Elektronen-Synchrotron DESY, Hamburg, Germany

(Received 18 June 1973)

The differential cross section for Delbrück scattering has been measured at photon energies between 1 and 7 GeV and scattering angles between 1 and 3 mrad on copper, silver, gold, and uranium targets. The results confirm the predictions of quantum electrodynamics, if the exchange of a very large number of photons with the nucleus (Coulomb correction) is taken into account. At momentum transfers of a few MeV/c, the Coulomb correction for uranium results in a reduction of the cross section by a factor between 3 and 5 as compared to the prediction of lowest-order relativistic perturbation theory. The photon-splitting process has been experimentally detected at the same energies and angles. Estimates of the cross section are given.

INTRODUCTION

Delbrück scattering[1] is the elastic scattering of photons in the Coulomb field of nuclei via virtual electron-positron pairs. It is one of the nonlinear processes in quantum electrodynamics which are a direct consequence of vacuum polarization. They are characterized by closed fermion loops in the corresponding Feynman diagram. These effects are forbidden within the framework of Maxwell's classical electrodynamics as a result of the linear form of its field equations and the principle of superposition. Besides Delbrück scattering there are some other processes, which are related to vacuum polarization; of these we only mention the scattering of light by light and the splitting of one photon into two by interaction with external fields. Their relationship becomes clear by looking at the corresponding Feynman diagrams in Fig. 1.

The scattering of light by light has been of particular interest for a long time, being a new process brought up by quantum electrodynamics. But up to now an experimental detection of scattering of light by light has not been possible because of the extremely small cross section and the difficulty of producing dense targets. Delbrück scattering is a first approximation to the scattering of light by light, in that one ingoing and one outgoing photon are replaced by virtual photons originating from the Coulomb field of a nucleus. This process is easier to measure, since one can use solid targets of high-Z material.

Delbrück scattering is of rather high order in the electromagnetic coupling constant. There are at least two photons exchanged with the nucleus due to the Furry theorem,[2] according to which diagrams containing fermion loops with an odd number of corners do not contribute to cross sections. This means that one-photon exchange does not contribute to Delbrück scattering. Thus the lowest-order nonvanishing Feynman diagram is of sixth order, which is fairly high compared to more common processes like bremsstrahlung and pair production which are of third order only. Thus it is possible to test the reliability of perturbation theory at higher orders by a measurement of Delbrück scattering.

Early approximate calculations of the Delbrück cross section[3,4] were based on the fact that Delbrück scattering is actually the shadow scattering of photons on nuclei which is due to photon absorption by electromagnetic pair production. The imaginary part of the forward Delbrück amplitude is related to the total pair-production cross section by the optical theorem. Starting from the known pair-production cross section Bethe and Rohrlich[4] in 1952 calculated the imaginary part of the Delbrück amplitude from the optical theorem and the real part via dispersion relations. These calculations gave results for small momentum transfers and high energies.

It was only recently that Cheng and Wu[5] (called CW I in the following) published calculations of the Delbrück cross section obtained via conventional perturbation theory. This calculation is valid for asymptotically high energies and not too small momentum transfers. At a momentum transfer of 0.5 MeV/c the cross section of CW I is a factor of two larger than the result of Bethe and Rohrlich. The cross section of CW I in Fig. 2 shows a strong forward maximum for the Delbrück cross section. Due to the two virtual photons exchanged with the nucleus the cross section is expected to be proportional to Z^4 and dominates over all competing elastic scattering processes for large Z and small angles.

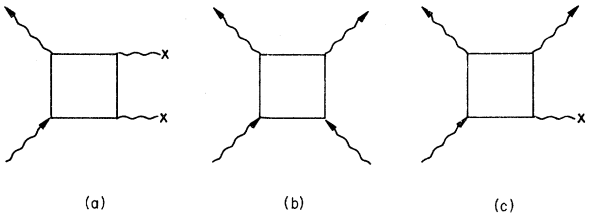

FIG. 1. Feynman diagrams for (a) Delbrück scattering, (b) the scattering of light by light, and (c) the photon-splitting process.

Although the existence of the Delbrück effect has already been predicted 40 years ago, there are very few clear observations and measurements of differential cross sections.[6,7] Most of these experiments had been performed in the energy range of nuclear physics, where it is difficult to separate the Delbrück effect from Rayleigh scattering which is not very well known quantitatively. Working at higher photon energies has the advantage that one is free from this complication. However, one has the difficulty of measuring at very small angles, where the Delbrück cross section is large enough to dominate over competing processes, mainly Compton scattering from electrons. At photon energies of a few GeV one has to measure scattered photons at a few milliradians to the primary beam (see Fig. 2).

One experiment has been performed at higher energies by Moffat and Stringfellow,[7] who used a 87-MeV bremsstrahlung beam. They clearly detected the Delbrück effect. However, the cross section measured by them cannot be used to discriminate between the predictions by Bethe and Rohrlich[4] and Cheng and Wu,[5] since in this experiment the contribution of degraded photons from showers developing in the target was not completely clear. Therefore it seemed worthwhile to perform another measurement in the GeV region, where the competing processes are well known.

Photon splitting, which is an inelastic scattering process of photons on nuclei, could possibly interfere with a measurement of the Delbrück effect. Like Delbrück scattering it is a high-order nonlinear effect in quantum electrodynamics, as is demonstrated by its Feynman diagram in Fig. 1. The primary photon is split into two outgoing ones by the interaction with the static Coulomb field of the target nuclei. Since there is only one photon exchanged with the nucleus, the cross section is proportional to Z^2. The energy of the primary photon is distributed between the two outgoing photons according to a distribution function, the form of which is not known for high primary energies. However, it has been shown[8] that the

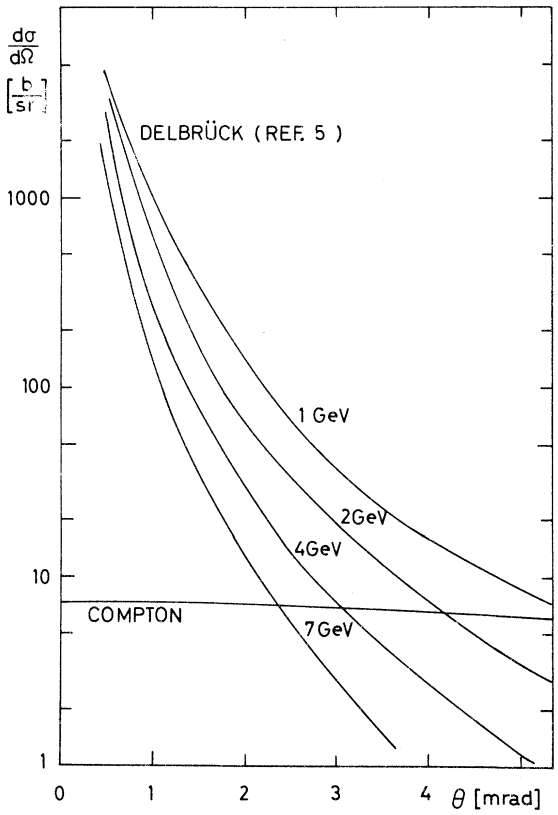

FIG. 2. Differential cross section $d\sigma/d\Omega$ for Delbrück scattering[5] and Compton scattering on uranium.

cross section for photon splitting goes linearly to zero as the energy of one of the outgoing photons approaches the primary energy. There is no infrared divergency in this case, since photon splitting is not a radiative correction, the corresponding elastic process being forbidden by Furry's theorem. It is this property which allows one to separate experimentally elastic Delbrück scattering from the inelastic photon-splitting contribution.

Estimates on the total cross section for photon splitting have been given by Bolsterli[9] and Bukhvostov.[10] The results of these authors differ by about an order of magnitude. Formulas for the differential cross section have been published by Shima[11] and Constantini *et al.*,[12] but have not been evaluated numerically or integrated for high energies because of their complicated structure.

Experimental data on photon splitting have been very scarce thus far. There is only one published experiment, by Adler and Cohen,[13] which was performed at 1.1-MeV photon energy. Their cross section comes out to be a factor of 5 larger than predicted by the theory. The need for more detailed measurements is obvious.

MEASURING METHOD

The experiment we report on was designed to measure small-angle elastic scattering of high-energy photons on heavy nuclei. The energy of the photons varied from 1 to 7.3 GeV. Scattered photons were detected in the angular range from 1 to 3 mrad. For target materials we used copper, silver, gold, and uranium.

The experimental setup is shown in Fig. 3. We used a well-collimated bremsstrahlung beam from the DESY electron synchrotron. The beam hit the scattering target, then passed without interaction through a magnetic pair spectrometer, and was finally buried in a quantameter serving as a monitor. There were several collimators and sweeping magnets cleaning charged particles from the beam. The scattered photons were converted into electron-positron pairs by a ring-shaped converter in front of the pair spectrometer which measured the photon energy and the coordinates of the conversion point of the photon.

The ability to measure scattered photons from the target at a few mrad relative to the primary beam places severe conditions on the quality of the photon beam as to beam divergence, beam spot size, and beam halo. We used a beam spot size at the scattering target of 6×6 mm^2, corresponding to a geometrical primary-beam divergence of ±0.15 mrad. The distance between target and pair converter was 20 m. A photon scattered by 1 mrad was 2 cm off the beam axis at the position of the converter, and the beam spot at this point was 8×8 mm^2. For the detection of scattered photons at the rate predicted for Delbrück scattering, the photon density of the primary beam had to be lowered by at least eight orders of magnitude when going from the beam axis to the inner radius of the converter ring.

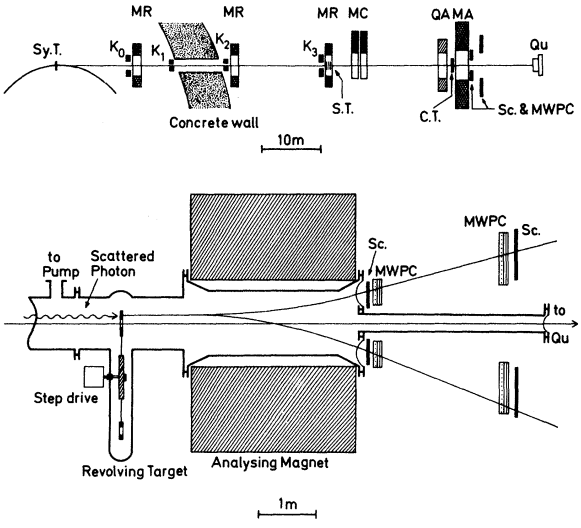

FIG. 3. Experimental setup. Legend:

Sy.T. = synchrotron target;
$K_0 - K_3$ = collimators;
MC, MR, QA = sweeping magnets;
S.T. = scattering target;
C.T. = converter target;
Sc. = scintillation counters;
M.W.P.C. = multiwire proportional chambers;
Qu = quantameter.

This reduction of the beam halo was achieved by a special system of collimators and sweeping magnets. Position and width of the collimators are given by the following consideration. The defining collimator in the beam line was the first one. All the following collimators were placed there to strip off the beam halo. They were not allowed to touch the primary beam again. Thus the edges of the second collimator were not to see the beam spot on the synchrotron target. The third collimator was not to touch the secondary beams emerging from the edges of the first collimator. The scattering target was placed immediately behind the third collimator. The inner edge of the conversion ring in front of the pair spectrometer was positioned so that it could not see either the synchrotron target or any edges of collimators except the last ones. Behind each collimator and the scattering target there were strong sweeping magnets which bent charged particles from the beam onto concrete shielding blocks. From the scattering target to the quantameter the photon beam was conducted in a vacuum tube to further reduce background and suppress spurious pair production. With this beam the empty-target background in our measurements was typically 30% of the total rate (see Tables I to IV for details).

Special attention was paid to the layout of the scattering target as a possible source of serious background of secondary photons. These secondary photons originated from bremsstrahlung produced by electron-positron pairs generated in the target by the primary beam. Their number rose as the square of the target thickness, since they were produced in a two-step process. In order to reduce this effect the target was split into several thin slices, each about 2×10^{-2} radiation length, which were placed one behind the other inside a sweeping magnet, with equal distances in between. The electron pairs created in one foil were deflected by the magnetic field on their path to the next foil, so that bremsstrahlung emitted in the following foils fell outside the angular acceptance of the pair spectrometer. Subdividing of the target into ten slices improved our signal-to-background ratio by an order of magnitude. The effect of this

TABLE I. Uranium data for Delbrück scattering.

k (GeV)	Θ (mrad)	Δ (MeV/c)	$\frac{d\sigma}{dt}$ (b/GeV^2)	Number of detected events	% Background	% Sec. phot.	% Compton	% Delbrück	Target (g/cm^2)	$Q_{\text{eff}}/10^{12}$
0.96	1.05	1.01	1145.0 ± 99.0	153	1.0	2.5	1.9	94.6	2.59	0.39
0.96	1.69	1.62	464.0 ± 29.0	372	10.7	3.5	3.7	82.1	2.59	0.84
0.96	2.23	2.14	100.0 ± 13.4	106	1.0	10.5	15.0	73.5	2.59	0.84
1.92	1.05	2.02	142.5 ± 14.5	129	9.1	5.2	2.7	83.0	2.59	0.94
1.92	1.69	3.24	38.0 ± 3.0	252	10.3	6.6	8.4	74.7	2.59	1.88
1.92	2.23	4.28	14.8 ± 1.9	120	3.3	7.3	18.0	71.4	2.59	1.88
1.92	2.75	5.28	6.8 ± 1.34	88	24.1	5.2	20.5	50.2	2.59	1.88
3.90	1.69	6.59	2.66 ± 0.28	269	19.4	6.8	17.7	56.1	1.65	9.16
3.90	2.23	8.70	0.78 ± 0.18	128	35.4	4.1	24.5	36.	1.65	9.16
3.90	2.75	10.70	0.50 ± 0.17	81	40.7	2.4	18.6	38.3	1.65	9.16
7.11	1.05	7.46	1.01 ± 0.34	43	39.1	8.0	11.	41.9	0.93	2.77
7.11	1.69	12.0	0.40 ± 0.05	252	23.0	2.5	21.	53.5	0.93	15.4
7.11	2.23	15.9	0.12 ± 0.02	90	25.6	1.8	18.9	53.7	0.93	15.4
7.11	2.75	19.6	$(5.9 \pm 1.4)10^{-2}$	48	23.1	2.1	4.4	70.4	0.93	15.4

TABLE II. Gold data for Delbrück scattering. (Data in parenthesis refer to double-thickness targets.)

k (GeV)	Θ (mrad)	Δ (MeV/c)	$\frac{d\sigma}{dt}$ (b/GeV^2)	Number of detected events	% Background	% Sec. phot.	% Compton	% Delbrück	Target (g/cm^2)	$Q_{\text{eff}}/10^{12}$
0.96	1.05	1.01	840.0 ± 74.0	143	1.0	1.1	2.2	95.7	0.91	0.95
0.96	1.69	1.62	249.0 ± 23.4	484	23.2	1.4	5.5	69.9	0.91	2.81
0.96	2.23	2.14	57.5 ± 6.9	133	1.0	3.1	23.8	72.1	0.91	2.81
0.96	2.75	2.64	25.1 ± 7.4	92	31.8	2.0	24.7	41.5	0.91	2.81
1.92	1.05	2.02	94.4 ± 11.7	107	22.7	1.2	3.0	73.1	0.91	1.96
			(89.5 ± 12.0)	96	(9.0)	(3.6)	(3.8)	(83.6)	(1.86)	(1.03)
1.92	1.69	3.24	18.4 ± 2.3	242	32.5	1.1	11.1	55.4	0.91	5.70
			(17.8 ± 2.3)	128	(20.5)	(4.0)	(13.1)	(62.4)	(1.86)	(1.03)
1.92	2.23	4.28	9.9 ± 1.2	142	8.6	.7	22.2	68.5	0.91	5.70
			(9.6 ± 1.5)	74	(5.2)	(2.7)	(22.9)	(69.8)	(1.86)	(1.03)
1.92	2.75	5.28	1.6 ± 1.3	87	70.2	.3	18.	11.5	0.91	5.70
			(2.5 ± 1.1)	45	(45.5)	(1.6)	(26.1)	(26.8)	(1.86)	(1.03)
3.90	1.69	6.59	1.9 ± 0.36	554	42.0	0.4	15.7	41.9	0.46	41.1
7.11	1.69	12.0	0.24 ± 0.08	476	70.0	0.2	10.7	19.1	0.28	56.2

TABLE III. Copper data for Delbrück scattering.

k (GeV)	Θ (mrad)	Δ (MeV/c)	$\frac{d\sigma}{dt}$ (b/GeV^2)	Number of detected events	% Background	% Sec. phot.	% Compton	% Delbrück	Target (g/cm^2)	$Q_{\text{eff}}/10^{12}$
1.92	1.69	3.24	0.61 ± 0.31	117	45.7	1.5	36.6	16.2	1.98	3.74
1.92	2.23	4.28	0.36 ± 0.20	78	10.0	1.0	68.4	20.6	1.98	3.74

target system on the counting rate in a given momentum acceptance of the pair spectrometer is demonstrated in Fig. 4.

Scattered photons were detected with the pair spectrometer. The photons hit a ring made of 2-mm aluminum, through the central hole of which the primary beam passed. The ring converted a definite fraction of the scattered photons into electron-positron pairs, which were bent by the magnetic field of the pair spectrometer and detected by scintillation counters and Charpak chambers. There was one telescope consisting of two scintillation counters and two Charpak chambers on the electron side of the spectrometer, and an identical one on the positron side placed symmetrically to the beam line behind the magnet. Each telescope accepted charged particles with momenta roughly between 35% and 70% of the maximum beam energy with the magnet setting used.

Coincidence of all four scintillation counters defined a trigger. The Charpak chambers were used for a complete reconstruction of the event that produced the trigger. In each Charpak chamber position there were two crossed wire planes installed to measure both coordinates of the charged particles passing through. A total of 1000 wires was used with a wire spacing of 2 mm, giving a space resolution of ±1 mm. The detection efficiency of the chambers was measured to be better than 99.5% at a time resolution of 120 nsec. The gas filling consisted of argon with 5% propane admixture. Signals from the proportional wires were amplified individually and strobed into flip-flops by the trigger pulse. The stored information was then automatically read into a small on-line computer, which served as data buffer and link to a large computer doing the final analysis. Details of the experimental apparatus will be published elsewhere.

Each particle track was defined by two points in space as measured by the Charpak chambers behind the pair-spectrometer magnet. Assuming the particle track to point to the center of the scattering target before entering the magnet, we were able to determine its bending angle as well as the coordinates of its conversion point. The momentum resolution came out to be 1%; the space resolution on the pair converter was ± 3 mm.

Both electron and positron of a pair must start from the same point on the conversion target within reconstruction errors. Applying this constraint we were able to eliminate spurious tracks and accidentals from the data. Reconstruction of the starting points of pairs on the converter gave us directly the scattering angle of the photon. The angular resolution was ±0.25 mrad given by the combined effect of reconstruction errors, beam-spot size, and primary-beam divergence. Photon energies were measured from the maximum bremsstrahlung energy E_0 down to $0.75E_0$ with 1% resolution.

The primary beam was buried in a total absorption ionization chamber, in our case a quantameter of the Wilson type, [14] which served as the absolute monitor for the beam intensity. Counting rates were normalized to the number of primary photons as given by the quantameter reading. Corrections have been applied for losses due to the measured dead time of the detection apparatus and the calculated absorption of photons in the scattering target.

To check the over-all performance and stability of the apparatus we have measured bremsstrahlung spectra at the beginning and end of each data-

TABLE IV. Silver data for Delbrück scattering.

k (GeV)	Θ (mrad)	Δ (MeV/c)	$\frac{d\sigma}{dt}$ (b/GeV^2)	Number of detected events	% Background	% Sec. phot.	% Compton	% Delbrück	Target (g/cm^2)	$Q_{\text{eff}}/10^{12}$
1.92	1.69	3.24	3.66 ± 0.70	213	41.6	1.0	20.8	36.6	1.20	7.09
1.92	2.23	4.28	2.80 ± 0.44	154	9.9	0.6	36.1	53.4	1.20	7.09
1.92	2.75	5.28	0.49 ± 0.50	116	66.0	0.2	25.2	8.6	1.20	7.09

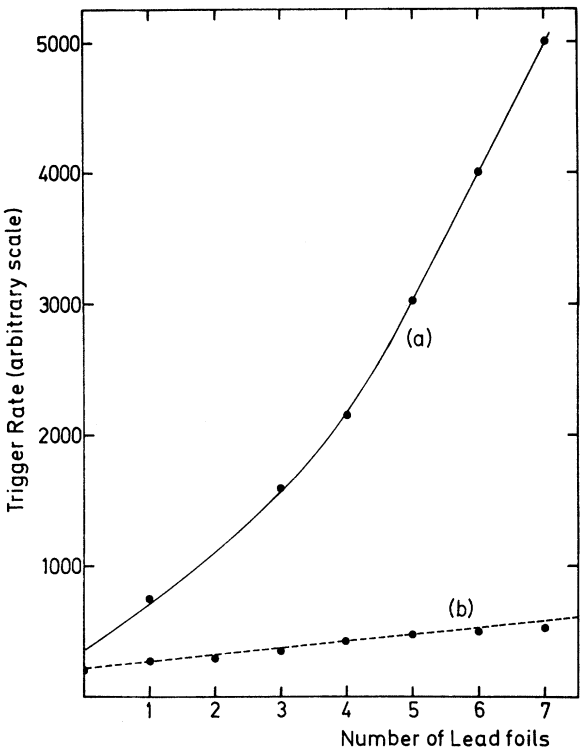

FIG. 4. Total trigger rate with the scattering target magnetic field (a) off and (b) on as a function of the number of target slices.

taking period using a conversion foil in front of the pair spectrometer instead of the ring and an empty scattering target. Within 4% the measured spectra agreed with absolute theoretical predictions. This agreement is satisfactory and provided us with information about the absolute precision of data measured with this apparatus.

DATA ANALYSIS

Spectra of scattered photons have been measured at maximum bremsstrahlung energies E_0 of 1, 2, 4, and 7.3 GeV with targets of copper, silver, gold, and uranium. Polar scattering angles have been accepted from 0.9 to 2.9 mrad over 2π azimuthal angle. Raw data have been normalized to the number of primary photons and corrected for pair-spectrometer efficiency, the latter one being calculated for each event according to its conversion point and energy. The data for each value of E_0 and each target material have been subdivided into four bins of polar angle and bins of 3% width of the photon energy.

After subtraction of empty-target background the spectra of scattered photons in each angular bin have been analyzed by a superposition of four processes:

(1) Delbrück scattering,
(2) Compton scattering on electrons,
(3) secondary photons from showers, and
(4) photon splitting.

Other processes one might think of, e.g., Compton scattering on nuclei, or forward photoproduction of neutral pions, have been estimated to give only a negligible contribution to the counting rate in our setup.

Two of the considered processes, i.e., (3) and (4), are inelastic and do not contribute to the counting rate at the edge of the bremsstrahlung spectrum. Thus, if one uses only photons from a narrow region at the maximum photon energy one measures essentially Delbrück and Compton scattering only. Compromising between the requirements of good statistics and low inelastic background we decided to use a 3%-wide energy bin just below E_0 for the evaluation of the Delbrück cross section. Corrections for inelastic contributions are small in this region, and the Compton contribution, being also small in most cases, is theoretically well known and can be easily subtracted.

In spite of the fact that we used only this 3% bin for determining the Delbrück cross section, we extended our analysis to the full accepted photon energy range of 25% below E_0 in order to be able to determine more reliable inelastic corrections and to look for photon splitting.

The procedure of the analysis is demonstrated by a typical example, the scattering of a bremsstrahlung beam of 1.95-GeV maximum energy on a gold target. The spectra shown in Fig. 5 apply to the angular bin 1.4 to 1.9 mrad. The normalized measured spectrum after subtraction of empty target background is shown in Fig. 5(a). There is a much steeper rise of the counting rate with decreasing energy than in a normal bremsstrahlung spectrum.

The contribution of secondary photons to this spectrum has been calculated by Monte Carlo methods from the known cross sections of pair production and bremsstrahlung to be given by the long-dashed line in Fig. 5(a). It amounts to 2% of the counting rate in the Delbrück bin, but is rising fast towards lower energies.

For checking experimentally the correct description of secondary photons by the Monte Carlo method, we varied the thickness of the scattering foils by a factor of two. Figure 6 shows the ratio between counting rates for double-thickness and single-thickness gold foils versus photon energy. For elementary processes this ratio would be 2. If secondary processes are present it comes out larger than 2. As expected, there are only

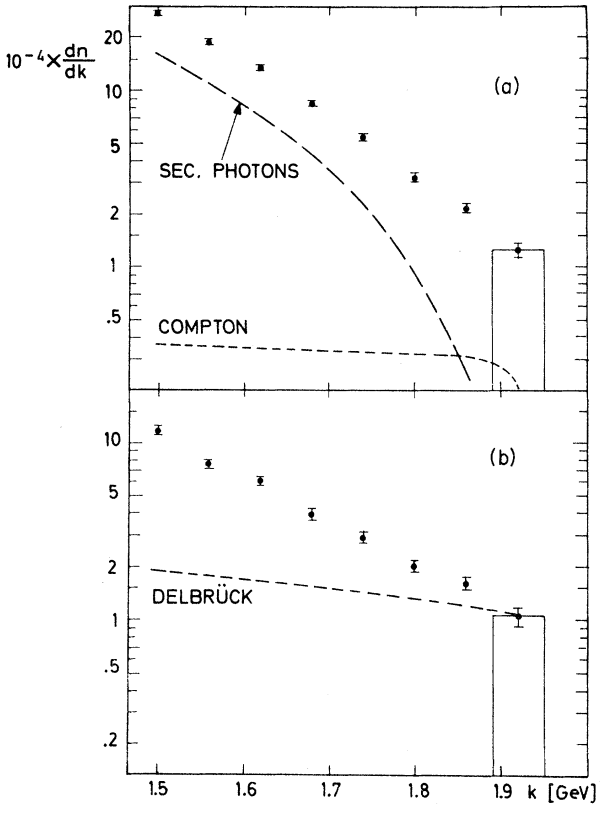

FIG. 5. (a) Normalized measured photon spectrum after subtraction of empty-target background for the scattering of a bremsstrahlung beam with 1.95-GeV maximum energy on a gold target. Long-dash line = calculated secondary photon contribution; short-dash line = calculated Compton contribution. (b) Experimental spectrum after subtraction of secondary photons and Compton-scattered photons. Long-dash line = contribution of elastically scattered photons.

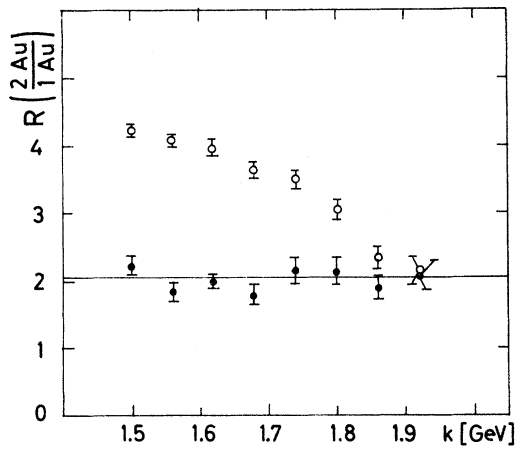

FIG. 6. Ratio of counting rates for gold foils with a thickness ratio 2.04 : 1.0. Open points refer to the total rate, full points to the rates after subtraction of secondary photons.

elementary processes contributing at the edge of the bremsstrahlung spectrum. At lower energies there is an appreciable contribution from secondary processes, but after subtraction of the Monte Carlo–simulated secondary photons there are only elementary processes left within the full energy range considered. That means that the Monte Carlo simulation of secondary photons is essentially correct over the full energy range.

The Compton contribution to the measured spectra has been calculated according to the formula of Klein and Nishina.[15] It is shown in Fig. 5(a) as the short-dash line. There is a decrease in energy of Compton-scattered photons depending on the scattering angle due to Compton kinematics. Within our angular range this decrease in photon energy is not sufficient to remove the Compton-scattered photons completely from the Delbrück bin. In the example of Fig. 5 the Compton contribution to the counting rate in the Delbrück bin amounts to 16% only.

In Fig. 5(b) the measured spectrum is shown after subtraction of secondary and Compton photons. Here the counting rate at the edge of the bremsstrahlung spectrum is assumed to be purely elastic and due to Delbrück scattered photons only. It will be shown later that this assumption is correct to 5%.

In order to identify the elastic contribution in the other parts of the spectrum, we varied the maximum energy of the bremsstrahlung spectrum experimentally. We find the broken line in Fig. 5(b) to be the elastic, i.e., the Delbrück, contribution to the counting rate. We see that with growing distance from the maximum energy the counting rate is increasing much faster than expected from the elastic contribution alone. What we know from the extra photons responsible for the steep rise in the soft part of the spectrum is that they are inelastically scattered photons originating from an elementary process in the target. Tentatively we assume these photons to be due to the photon-splitting process.

RESULTS ON DELBRÜCK SCATTERING

All results on Delbrück scattering given in this section are based on an analysis of events with photon energies larger than $0.97E_0$ with the corrections applied as described before. Cross sections have been evaluated by comparing Monte Carlo–simulated event rates with the observed ones, thus taking into account the finite experimental resolution in energy and angle. The theoretical Delbrück cross section has been used for the simulation. The resulting measured differen-

tial cross sections are summarized in Tables I to IV. Quoted errors are statistical ones. Systematic errors have been neglected since they are much smaller than the statistical ones in all cases.

Considering only the lowest-order contribution from the relativistic perturbation theory one expects a Z^4 dependence of the Delbrück cross section. We have checked this prediction by plotting the Z dependence of the measured cross section in Fig. 7. The experimental points are roughly compatible with a Z^4 behavior, but are consistently lower than the theoretical prediction.

At this point there was the suspicion that higher-order effects might be responsible for this result. The effective coupling constant of the virtual electron or positron to the target nucleus is $Z\alpha$, which for large Z is no longer small compared to unity. The Born approximation breaks down there, as is well known for pair production and bremsstrahlung, where the actual cross section for lead is about 10% less than the Born approximation predicts. This can be repaired by the so-called Coulomb correction, which in the picture of Feynman diagrams means that one has to take into account the exchange of an infinite number of virtual photons between electron and nucleus. Cheng and Wu[16] introduced the Coulomb correction into their Delbrück cross section. We have integrated their formula by a Monte Carlo technique and indeed got an impressive reduction of the cross section as compared to the Born approximation. The broken line in Fig. 7 shows the new theoretical prediction. It comes much closer to the experimental values.

Figures 8 and 9 show our complete results on the Delbrück cross section for gold and uranium as targets, compared to the theoretical prediction with and without Coulomb correction. They confirm in detail what has been discussed before. The measured values are a factor of 2 to 7 below the Born approximation, depending on momentum transfer and atomic number, but they are essentially in agreement with the theory including the Coulomb correction. Thus the Delbrück cross section is drastically modified by the Coulomb correction. To our knowledge this is the largest effect ever observed for this kind of higher-order corrections.

A closer inspection of our data reveals that there might be systematic deviations present even from the improved theoretical curve, but our statistical errors do not allow a definite statement on this point.

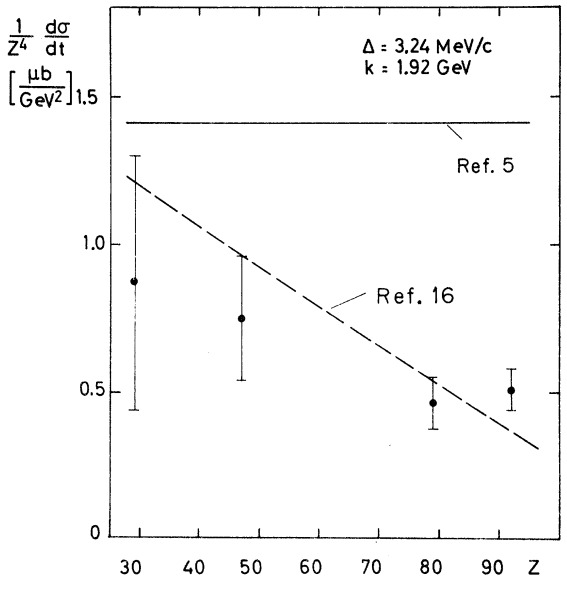

FIG. 7. Measured cross section for Delbrück scattering for fixed momentum transfer as a function of the atomic number Z. The full curve represents the prediction of Ref. 5; the long-dash line refers to Ref. 16.

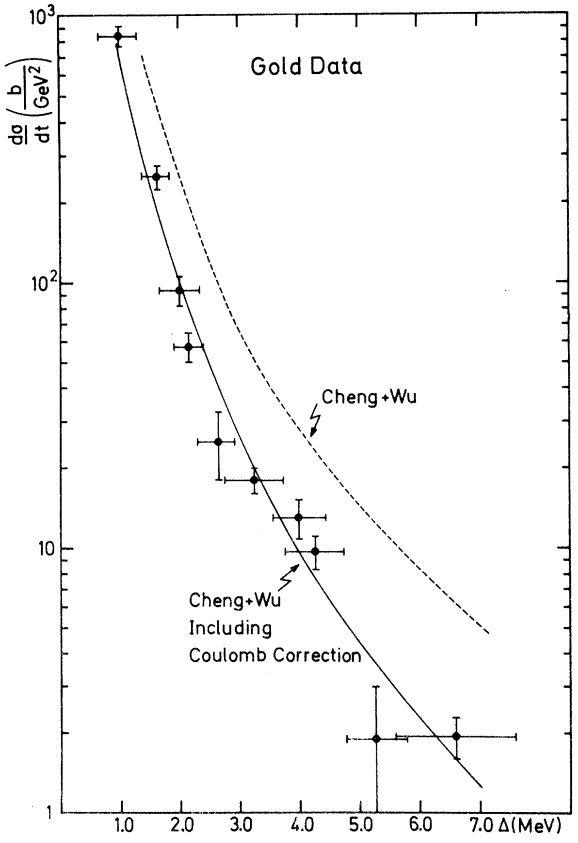

FIG. 8. Measured differential cross sections for Delbrück scattering versus momentum transfer for gold targets compared to theoretical predictions.[5,16]

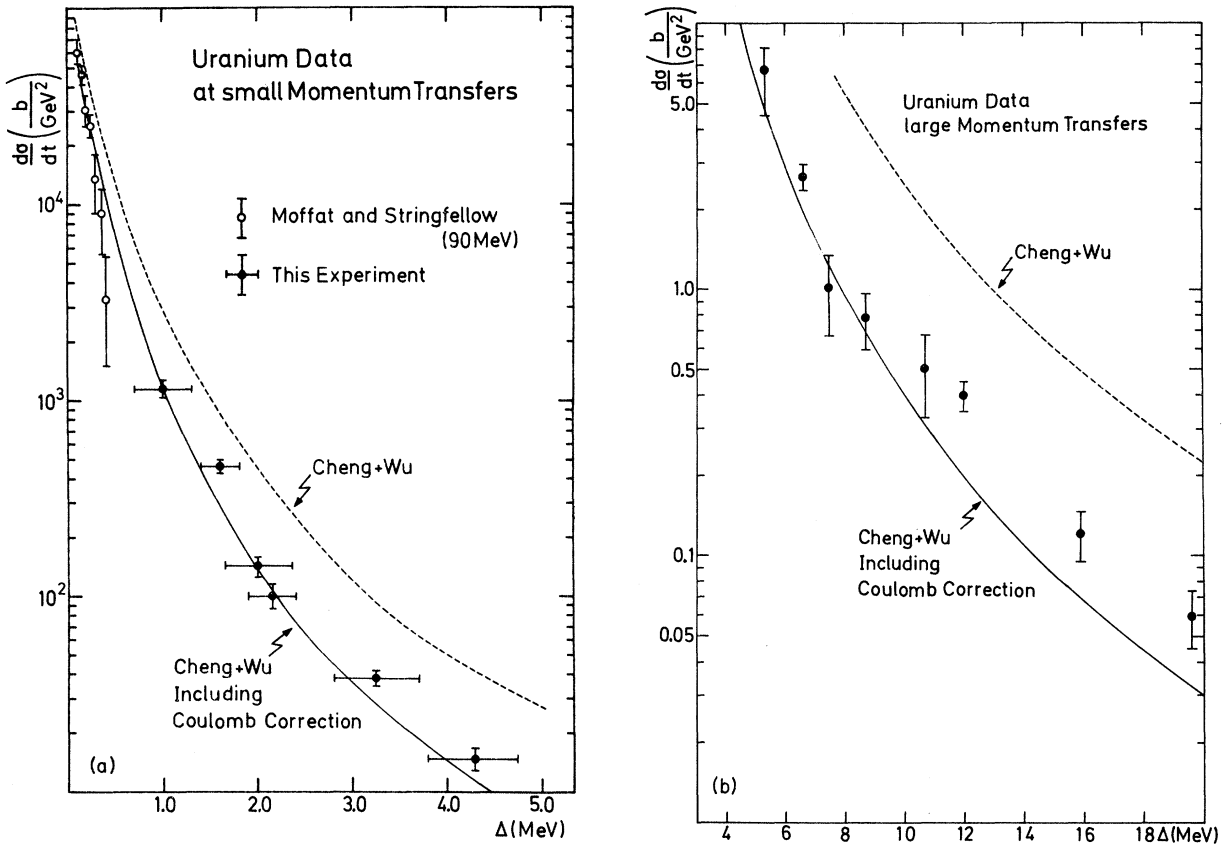

FIG. 9. Measured differential cross sections for Delbrück scattering versus momentum transfer for uranium targets compared to theoretical predictions (Refs. 5 and 16). (a) Small momentum transfers; (b) large momentum transfers.

RESULTS ON PHOTON SPLITTING

It has been shown before that the low-energy part of the measured photon spectra cannot be explained as a superposition of Delbrück scattering, secondary photons, and Compton scattering alone.

There is a strong contribution from inelastically scattered photons which we attribute to the photon-splitting process. To check this assumption we have plotted in Fig. 10 the number of these photons divided by Z^2 versus Z. Within errors the result is independent of Z, which means that the cross section of the process producing these photons is proportional to Z^2. This is exactly what one would expect for photon splitting. We take the observed Z^2 dependence together with the fact that the process is inelastic and elementary as evidence that photon splitting has been observed.

The evaluation of cross sections for photon splitting from our data is complicated by two facts: (1) Since we use a bremsstrahlung beam the incident photon energy is not known. (2) The final

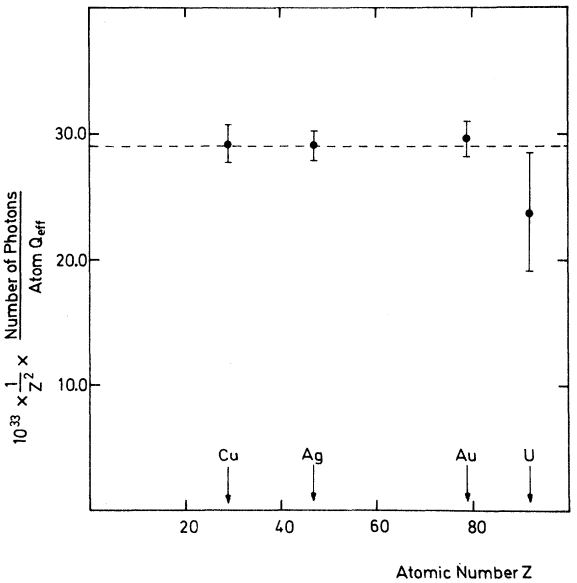

FIG. 10. Total number of detected photons exceeding the contribution of Delbrück scattering, secondary photons, and Compton scattering divided by Z^2 versus Z.

state of photon-splitting events contains two photons. Only one of these is completely analyzed by our apparatus. The counting rate of photon splitting in our experiment is given by the following integral:

$$R(k_1) = \int_{k_1}^{E_0} \frac{dn}{dk} dk \times 2N \frac{d\sigma(k, k_1)}{d\Omega_1 dk_1} \Delta\Omega_1 \Delta k_1 ,$$

where

k is the energy of the primary photon,
k_1 is the energy of the detected photon,
dn/dk is the differential bremsstrahlung spectrum,
$d\sigma(k, k_1)/d\Omega_1 dk_1$ is the differential photon splitting cross section integrated over the angles of the second photon,
$\Delta\Omega_1$ is the accepted solid angle of photon k_1,
Δk_1 is the width of the momentum bin of k_1, and
N is the number of target atoms per cm^2.

The differential cross section for photon splitting as a function of k and k_1 cannot be extracted from this relation without additional assumptions on either the k or the k_1 dependence, both of which are not known *a priori*. Without such assumptions cross sections can be given for special pairs of k and k_1 only according to the following procedure: Dividing the accepted photon energy interval at each setting of the maximum bremsstrahlung energy into two halves, we take the number of split photons in the low-energy half to be produced by primary photons from the high-energy half. Taking the central energy value of the upper half to be the mean primary energy k and the central value of the lower half as the mean energy k_1 of the split photons, we get the cross section for photon splitting at k and k_1 averaged over energy intervals Δk and Δk_1, each about 15% wide. The results are shown in Fig. 11. There is a steep rise of the cross section with decreasing angle of the detected photon and with decreasing primary energy.

To check on systematic errors of the analysis we tried a quite different approach for the evaluation of photon-splitting cross sections, based on the assumption of a linear rise of the cross section with $k_2 = k - k_1$, as advocated by Sannikov.[8] By this method we find cross sections that are approximately 25% lower than those given in Fig. 11.

The differential cross sections for photon splitting as presented in Fig. 11 allow an estimate of the contamination of the Delbrück signal by photon-splitting events. The contamination comes out to be at most 5%. This is an upper limit, since we used the photon-splitting cross section at $k_1/k = 0.87$, whereas for the Delbrück bin $k_1/k = 0.99$ applies and the photon-splitting cross section must go to zero for $k_1/k \to 1$. As the statistical errors of the Delbrück cross section are generally larger than this contamination we have neglected it altogether.

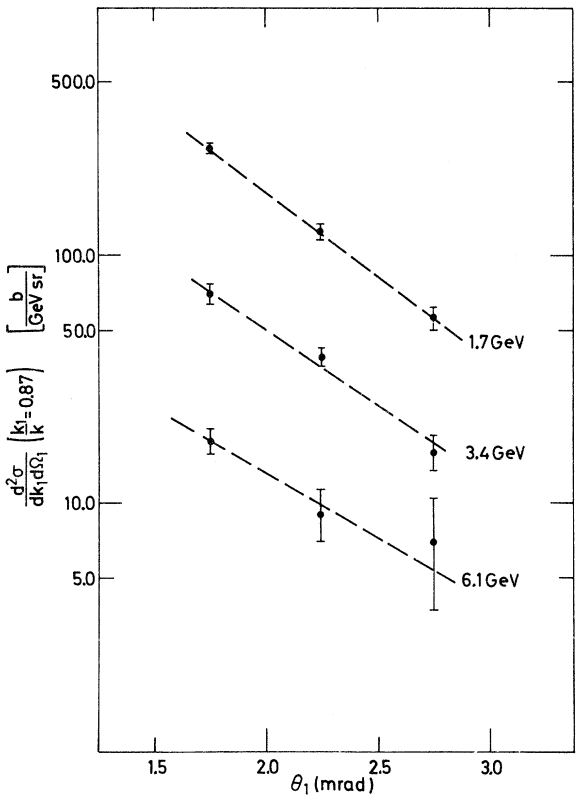

FIG. 11. Differential cross sections for photon splitting on gold. The lines are drawn to guide the eye.

For the comparison of our data on photon splitting with estimates of the total cross section existing in the literature we integrated our results over the accepted solid angle and energy of the split photons. The result is shown in Table V compared to predictions of Bolsterli[9] and Bukhvostov[10] for the total cross section. Considering the fact that in our experiment we integrate over a small part of the angular and energy ranges only both theoretical predictions seem to be low.

TABLE V. Integrated experimental cross sections for photon splitting on gold, compared to theoretical predictions for the *total* cross section.

k (GeV)	σ_{exp} (mb)	σ_{tot} (mb) (Ref. 9)	σ_{tot} (mb) (Ref. 10)
1.47 – 1.89	1.42 ± 0.05	0.78	4.8
3.00 – 3.84	0.80 ± 0.04	0.85	4.8
5.42 – 6.77	0.41 ± 0.03	0.91	4.8

CONCLUSION

The Delbrück cross section has been measured to be, for high energy, high Z, and for a few MeV/c momentum transfer, a factor 3 to 5 smaller than calculated in lowest nonvanishing order of perturbation theory. This drastic reduction is due to a special kind of higher-order corrections, the Coulomb correction, which fully accounts for the observed difference.

There is strong evidence for the photon-splitting process being present in our data. The cross section for photon splitting deduced from these data is of the expected order of magnitude, but at present there are no precise theoretical numbers to compare with. Experimentally the next step should be a coincidence experiment on the photon-splitting process; from our experience such an experiment is feasible.

ACKNOWLEDGMENTS

We wish to thank Professor E. Lohrmann for his encouragement and support for the experiment. The experiment would not have been possible without the help and effort of Professor P. Waloschek concerning our proportional chambers and the amplifiers used. In this respect we have to thank Mr. A. Krolzig and Mr. Pforte for their help on software and hardware problems. We thank the DESY-Hallendienst for its continuous and excellent support during the experiment. We thank Professor G. von Dardel and Dr. M. Wong for stimulating discussions in the early stage of the experiment. During the data analysis we had very helpful discussions with Professor T. T. Wu about the implications of our experiment. Finally we want to thank Dr. J. Thiem for his careful chemical analysis of our uranium targets.

---

*Present Address: CERN, Geneva, Switzerland.

[1]M. Delbrück, Z. Phys. 84, 144 (1933).
[2]W. H. Furry, Phys. Rev. 51, 125 (1937).
[3]F. Rohrlich and W. Gluckstern, Phys. Rev. 86, 1 (1952); F. Rohrlich, *ibid.* 108, 169 (1957); P. Kessler, J. Phys. Radium 19, 739 (1958); W. Zernik, Phys. Rev. 120, 549 (1960); F. Ehlotzky and G. G. Sheppey, Nuovo Cimento 33, 1185 (1964).
[4]H. A. Bethe and F. Rohrlich, Phys. Rev. 86, 10 (1952).
[5]H. Cheng and T. T. Wu, Phys. Rev. 182, 1873 (1969); 182, 1899 (1969); Phys. Rev. Lett. 22, 666 (1969).
[6]R. Bösch *et al.*, Phys. Lett. 2, 16 (1962); R. Bösch *et al.*, Helv. Phys. Acta 36, 625 (1963); U. Stierlin *et al.*, Z. Phys. 170, 47 (1962); H. E. Jackson and K. J. Wetzel, Phys. Rev. Lett. 22, 1008 (1969).
[7]J. Moffatt and M. W. Stringfellow, Proc. R. Soc. Lond. A254, 242 (1960).
[8]S. S. Sannikov, Zh. Eksp. Teor. Fiz. 42, 282 (1962) [Sov. Phys.—JETP 15, 196 (1962)].
[9]M. Bolsterli, Phys. Rev. 94, 367 (1954).
[10]A. P. Bukhvostov *et al.*, Zh. Eksp. Teor. Fiz. 43, 655 (1962) [Sov. Phys.—JETP 16, 467 (1963)].
[11]Y. Shima, Phys. Rev. 142, 944 (1966).
[12]V. Constantini *et al.*, Nuovo Cimento 11A, 733 (1971).
[13]A. W. Adler and S. G. Cohen, Phys. Rev. 146, 1001 (1966).
[14]R. R. Wilson, Phys. Rev. 80, 720 (1953).
[15]O. Klein and Y. Nishina, Z. Phys. 52, 853 (1929).
[16]H. Cheng and T. T. Wu, DESY Report No. 71/69 (unpublished).